Reversal effects in stochastic kink dynamics

A. V. Savin,* G. P. Tsironis, and A. V. Zolotaryuk†
Physics Department, University of Crete, Greece and Foundation for Research and Technology–Hellas, Heraklion, Crete, Greece
(Received 27 March 1997)

We study collective regular and stochastic dynamics in a chain of harmonically coupled particles subjected to an on-site potential with two degenerate energy wells but with differing frequencies of small-amplitude oscillations at their minima. We identify and study asymmetry-induced properties of a Peierls-Nabarro relief, kink-antikink interactions, and stochastic kink motion. In particular, we predict analytically and confirm numerically directed noise-induced soliton motion when the chain particles are driven by white and exponentially correlated noise. The difference of frequencies of oscillations in the vicinity of the wells is shown to be a sufficient condition for the existence of such a directed kink motion. We find that under certain conditions a reversal of the soliton motion takes place; these conditions involve the noise properties such as a critical correlation time or noise strength or the presence of an external d.c. field. In particular, we find that above some critical value of temperature, the directed soliton transport occurs against an applied d.c. field. [S1063-651X(97)07508-9]

PACS number(s): 05.40.+j, 03.20.+i, 43.50.+y, 46.10.+z

I. INTRODUCTION

Since the pioneering work of Krumhansl and Schrieffer [1] and Aubry [2] on the dynamics of topological solitons (kinks and antikinks) in the ϕ^4 field theory, there has been great interest in applications of this theory in condensed matter physics and biology [3]. A chain of harmonically coupled particles each subjected to the local (on-site) symmetric double-well potential is adopted to be a basic model in these studies due to its simplicity as well as the existence of analytical soliton solutions. We note that the majority of materials with strong quasi-one-dimensional anisotropy admitting the existence of topological defects have indeed a relatively simple structure without any asymmetry of the on-site potential. For instance, in a hydrogen-bonded chain $(X\text{—H})_\infty$, where X is one of the atoms O, F, Cl, or Br, both the ground-state configurations $\cdots X\text{—H}\cdots X\text{—H}\cdots X\text{—H}\cdots$ and $\cdots \text{H—}X\cdots \text{H—}X\cdots \text{H—}X\cdots$ are completely equivalent, both energetically and structurally [4]. Asymmetry is absent in such systems and the top of the on-site double-well potential is situated at the midpoint of the hydrogen bond. However, topological defects can also exist in more complex condensed matter and biomolecular objects, e.g., in microtubules [5]. In the latter case, an electron moving in a tubulin dimer can reside in either tubulin monomer, viz., in the α or β monomer. The resulting two-minima relief separated by a maximum configuration of the electron dipole moment has been described through a symmetric double-well (ϕ^4) potential [5]. This model provides a simplification for the electron transfer process. One could argue that structural difference between the α and β tubulin monomers as well as the accompanying conformational changes of the β monomer while the electron resides in this monomer renders the system asymmetric. As a result, the model potential for the process is indeed bistable and asymmetric one. This structural asymmetry is not unexpected and it appears in other complex biomolecular systems where bistability is a result of the existence of pairs of similar but not identical building blocks.

Single-particle stochastic symmetry-breaking phenomena have recently seen an explosion of interest of physicists since their original appearance a few years ago in the context of molecular motors [6–13]. The symmetry-breaking effect involves a *directed* motion of a single particle in an *asymmetric periodic* potential under the influence of noise fluctuations that have some correlation property. The macroscopic manifestation of such a preferential motion of independent particles is through the appearance of a nonzero particle (probability) current. This *ratchet* effect seems to be generic in the context of single-particle stochastic dynamics in periodic but anisotropic (asymmetric) potentials [8]. Since the topological soliton state in the kink-bearing family can be considered simply as an effective single particle [14], it would be expected that the ratchet effect takes place also for solitons moving in an asymmetric periodic on-site potential. Recently, the stochastic ratchet effect has been extended to the soliton case [15,16]. Marchesoni in particular has shown that a stationary noise-induced current of kinks and antikinks in opposite directions exists as a function of the noise *correlation time* and the kink-antikink *asymmetry* [15].

The present paper aims to study in detail the regular and stochastic kink dynamics in the other class of kink-bearing models where the on-site potential is an asymmetric *double-well* function with *degenerate* minima [16]. More precisely, the asymmetry of the double-well potential means that the frequencies of small-amplitude oscillations at the potential minima are *different*. In such a case of bounded motion, no stationary current of kinks and antikinks in the same direction can exist as in the case of a periodic potential [15]. The basic question is now as to whether preferential kink (antikink) motion occurs as well as the detailed conditions for such directed kink (antikink) motion. We will show that such a motion does indeed take place not only with colored noise,

*Also at the Institute for Problems of Physics and Technology, 119034 Moscow, Russia.

†Also at the Bogolyubov Institute for Theoretical Physics, 252143 Kyev, Ukraine.

as in Ref. [15], but also in the presence of white noise. This result is not in contradiction with the second law of thermodynamics; it simply expresses the fact that our kink-bearing system is not truly in thermodynamic equilibrium.

The main point of our studies in this paper is to describe the factors that determine the direction of stochastic soliton motion. We find that there are three factors: (i) the correlation properties of the noise, (ii) the noise intensity, and (iii) the external dc field. By studying the different resulting regimes, we can find corresponding critical values at which the *reversal* of the kink (antikink) motion occurs. We note that the reversal of the directed single-particle motion in an asymmetric periodic potential is affected by the exact shape of the potential and especially its higher derivatives [17].

The paper is organized as follows. In the next section we describe the chain model with an asymmetric double-well on-site potential. Standing kink (antikink) solutions and the corresponding Peierls-Nabarro potential relief will be obtained in Sec. III. In Sec. IV we study the regular dynamics of asymmetric kinks and antikinks. In Sec. V we give the theory that allows the prediction of the direction of the stochastic soliton motion. This theory is confirmed by numerical simulations of the equations of motion in Sec. VI. Finally, we summarize our findings in Sec. VII.

II. AN ASYMMETRIC BISTABLE CHAIN MODEL

We consider a chain of harmonically coupled particles subjected to an on-site potential of a general form. This model belongs to the discrete nonlinear Klein-Gordon family, describing *topological* soliton dynamics in one-dimensional lattices. Its Hamiltonian has the standard form [1–3]

$$H=\sum_n \left[\frac{1}{2}\, m\dot{x}_n^2+\kappa(x_{n+1}-x_n)^2+\varepsilon_0 V(x_n/a)\right], \qquad (1)$$

where m is the mass of a chain particle, κ is the stiffness constant of the interparticle nearest-neighbor interaction, x_n is the displacement of the nth particle from the midpoint between the minima of the dimensionless on-site potential $V(u)$, a is the half distance between the minima, and the overdot denotes differentiation with respect to time t. In this paper we are dealing with the on-site potential function $V(u)$ of the double-well form with two energetically *degenerate* minima (ground states) and *differing* frequencies of small-amplitude oscillations at the minima. In what follows this potential is called an *asymmetric bistable* (AB) potential. More precisely, we define the on-site double-well function $V(u)$, $-\infty<u<\infty$, satisfying the following properties (see Fig. 1): (i) both its minima situated at the points $u=\pm 1$ are degenerate and (ii) its curvatures at the minima or, in other words, the frequencies of small-amplitude oscillations in the ground states $\Omega_1=\sqrt{V''(-1)}$ and $\Omega_2=\sqrt{V''(1)}$ are different, i.e., $V''(-1)\neq V''(1)$. Here and throughout the present paper primes denote differentiation. As shown in Fig. 1, we normalize the function $V(u)$ through $V(\pm 1)=0$ and $V(l_0)=1$, where $l_0\in(-1,1)$ is the position of the barrier top separated by the minima at the points $u=\pm 1$; therefore, the parameter ε_0 should be referred to as the barrier height of the on-site AB potential.

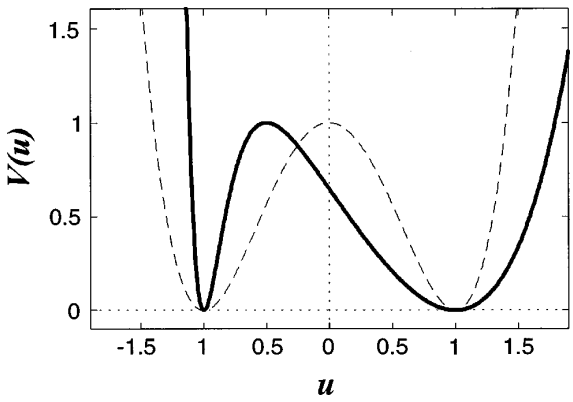

FIG. 1. Form of the AB potential $V(u)$ with the parameter values $b_1=0.5$ and $b_2=5$ (solid line). For comparison, the form of the symmetric double-well potential with $b_1=b_2=0.5$ is also presented (dashed line).

The function

$$V(u)=\left(\frac{1-\exp[b_1(u-1)]}{1-\exp[b_1(l_0-1)]}\,\frac{1-\exp[-b_2(u+1)]}{1-\exp[-b_2(l_0+1)]}\right)^2 \qquad (2)$$

can be chosen as the simplest example of the AB potential. Here the position of the barrier top l_0 is determined as a solution $u=l_0$ of the equation

$$\frac{\exp[b_1(1-u)]-1}{b_1}=\frac{\exp[b_2(1+u)]-1}{b_2}. \qquad (3)$$

It follows from Eq. (3) that the barrier top is shifted to the left ($l_0<0$) if $b_1<b_2$ and vice versa, it is shifted to the right ($l_0>0$) if $b_1>b_2$. In particular, we choose the values $b_1=0.5$ and $b_2=5.0$ and then we find that the frequency of the oscillations of the particle in the left well $\Omega_1=9.23$ exceeds the frequency of the oscillations in the right well $\Omega_2=1.46$ by one order. These parameter values are used throughout this paper in numerical computations. In the particular case $b_1=b_2=b$ we have $l_0=0$ and the function (2) is reduced to the symmetric form

$$V(u)=\left[\frac{\alpha-\cosh(bu)}{\alpha-1}\right]^2,\quad \alpha=\cosh b, \qquad (4)$$

used before in a number of studies on the proton transport in hydrogen-bonded chains [18,19]. In the limit $b\to 0$, the potential (4) takes the form of the well-known ϕ^4 potential $\lim_{b\to 0}V(u)=(1-u^2)^2$.

It is convenient to use the dimensionless time and lattice field according to

$$\tau=\sqrt{\varepsilon_0/m}\,t/a,\quad u_n(\tau)=x_n(t)/a, \qquad (5)$$

respectively. Then the Hamiltonian (1) can be rewritten in the dimensionless form as

$$\mathcal{H}=\frac{H}{\varepsilon_0}=\sum_n \left[\frac{1}{2}\left(\frac{du_n}{d\tau}\right)^2+\frac{1}{2}\, g(u_{n+1}-u_n)^2+V(u_n)\right] \qquad (6)$$

where the dimensionless ''cooperativity'' parameter $g=\kappa a^2/\varepsilon_0$ has been introduced to describe the magnitude of the interparticle interaction compared to the barrier height. We also call the parameter g the dimensionless intersite coupling.

When the AB chain is brought into contact with a stochastic bath, its dynamics is described by the system of the coupled Langevin equations

$$\frac{d^2u_n}{d\tau^2}=g(u_{n+1}-2u_n+u_{n-1})-V'(u_n)+f-\gamma\,\frac{du_n}{d\tau}+\eta_n,$$

$$n=0,\pm1,\pm2,\ldots, \quad (7)$$

written in the dimensionless form [see the Hamiltonian (6)]. Here f is a dimensionless constant external force, $\gamma=a\sqrt{m/\varepsilon_0}/\tau_r$ is the dimensionless friction coefficient with t_r being the relaxation time, and the dimensionless random force η_n describes the interaction of the nth chain particle with the stochastic bath. The forces η_n are supposed to be independent at differing chain sites and they are defined by the correlation functions

$$\langle\eta_{n_1}(\tau_1)\eta_{n_2}(\tau_2)\rangle=2D\gamma\delta_{n_1n_2}\varphi(\tau_1-\tau_2), \quad (8)$$

where D is the dimensionless noise strength and the autocorrelation function $\varphi(\tau)$ is normalized by $\int_{-\infty}^{\infty}\varphi(\tau)d\tau=1$. For white noise $\varphi(\tau)=\delta(\tau)$ ($D=k_BT/\varepsilon_0$, where k_B is Boltzmann's constant and T is the thermal bath temperature), whereas for the exponentially correlated noise

$$\varphi(\tau)=(\lambda/2)\exp(-\lambda|\tau|). \quad (9)$$

Here $\lambda=1/\tau_c$, with τ_c being the (dimensionless) correlation time of the random forces η_n.

III. STANDING SOLITON STATES AND A PEIERLS-NABARRO RELIEF

To find standing soliton (kink and antikink) profiles and the corresponding Peierls-Nabarro (PN) relief [20], we solve the minimization problem

$$\mathcal{E}=\sum_n\left[\frac{1}{2}\,g(u_{n+1}-u_n)^2+V(u_n)\right]\to\min_{u_2,\ldots,u_{N-1}}, \quad (10)$$

with the boundary conditions $u_1=-1$ and $u_N=1$ (kink) or $u_1=1$ and $u_N=-1$ (antikink). Numerically, it is convenient to define the soliton center position

$$n_c=\frac{1}{2}+\sum_{n=1}^{N-1}np_n \quad (11)$$

and the soliton width

$$\mathcal{D}=1+2\sqrt{\sum_{n=1}^{N-1}\left(n+\frac{1}{2}-n_c\right)^2p_n}, \quad (12)$$

where the sequence $p_n=|u_{n+1}-u_n|/2$, $n=1,\ldots,N-1$, describes the distribution of chain deformation.

The minimization problem (10) was solved numerically by the method of conjugated gradients for the chain consisting of 400 particles. The solution of this problem allows us to find only stable states of a standing kink (or antikink). Kink profiles can be obtained from antikink profiles simply by the symmetric mapping and their form is always asymmetric. To find other (unstable) kink profiles as well as a dependence of the kink energy on the position of its center, i.e., a PN relief, we fix a certain value $u_{N/2}\in(-1,1)$ (fixing by this a corresponding kink center n_c) and minimize the energy (10), assuming the rest of variables u_n to be free. Varying monotonically the variable $u_{N/2}$, we obtain a monotonic change of the kink position n_c (a kink center position is uniquely determined by $u_{N/2}$). As a result, one calculates the dependence $\mathcal{E}=\mathcal{E}(n_c)$.

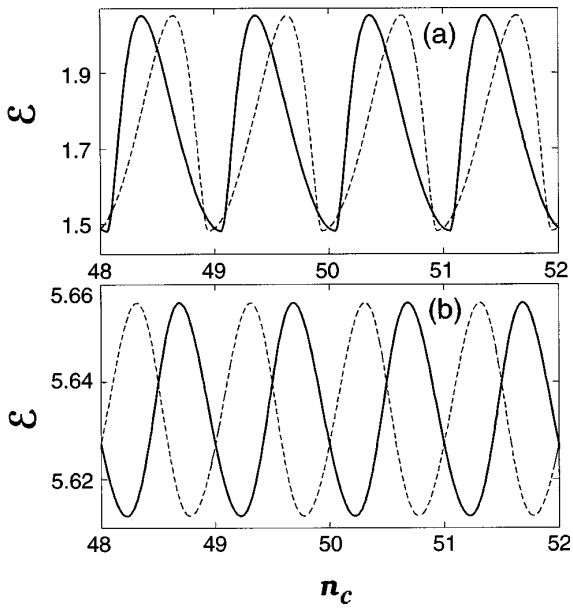

FIG. 2. PN potential relief $\mathcal{E}(n_c)$ for the antikink (solid line) and the kink (dashed line) for (a) $g=1$ and (b) $g=10$.

The solution of the minimization problem (10) has shown that the PN relief is a periodic potential with the period equal to 1, i.e., the chain spacing. The PN potential minima $e_1\pm n$ ($0\leqslant e_1<1$) correspond to stable states of the standing kink solution, while the maxima $e_2\pm n$ ($e_1\leqslant e_2<e_1+1$) are unstable kink states. The difference of these energies (i.e., the amplitude of the PN relief) $\Delta\mathcal{E}=\mathcal{E}(e_2)-\mathcal{E}(e_1)$ gives a pinning energy of the kink or antikink to the chain, viz., the activation energy for kink motion.

The PN relief for two cases $g=1$ and $g=10$ is shown in Fig. 2. For weak couplings ($g=1$), the relief $\mathcal{E}(n_c)$ has an *asymmetric* profile and the asymmetry practically vanishes with increasing the coupling g. It is useful to define the parameter of the relief asymmetry by $\sigma=2(e_2-e_1)-1$ ($-1\leqslant\sigma\leqslant1$). Thus, for the antikink in the chain with $g=1$, we have $e_1=0.06$, $e_2=0.36$, and $\sigma=-0.39$; in the case $g=10$, these parameters are $e_1=0.22$, $e_2=0.69$, and $\sigma=-0.07$. For the kink, the asymmetry of the potential relief has the other sign (the maxima are shifted to the right): $e_1=0.94$, $e_2=1.64$, and $\sigma=0.39$ if $g=1$ and $e_1=0.78$, $e_2=1.31$, and $\sigma=0.07$ if $g=10$.

The energy $\mathcal{E}(g)$ and the width $\mathcal{D}(g)$ of the standing kink (antikink) solution monotonically increase with the growth of the coupling parameter g (proportionally to $\sqrt{g}$), while the pinning energy $\Delta\mathcal{E}(g)$ exponentially tends to zero as illus-

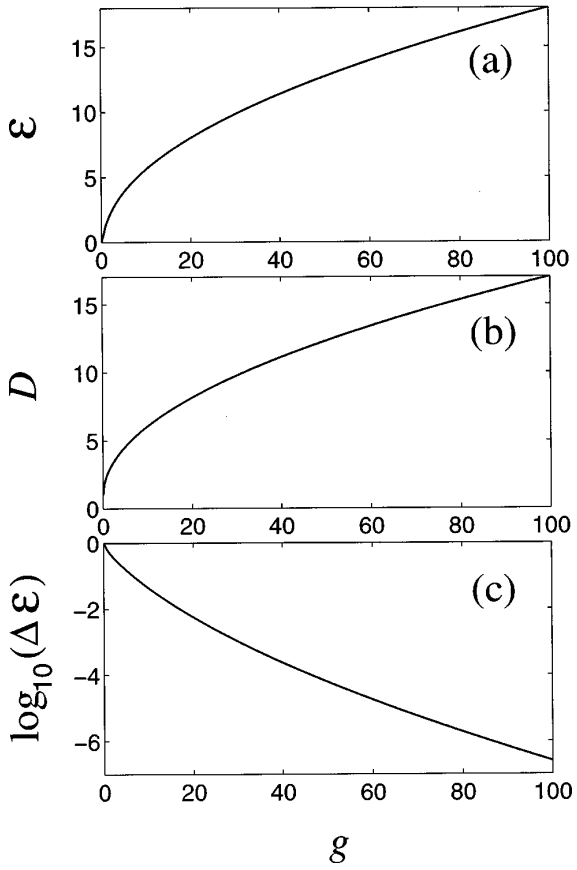

FIG. 3. Dependence of (a) the energy $\mathcal{E}$ of the stable standing kink state, (b) the kink width $\mathcal{D}$, and (c) the pinning energy $\Delta\mathcal{E}$ on the coupling parameter g.

trated in Fig. 3. In the chain with weak cooperativity g the kink (antikink) is pinned and requires the activation energy $\Delta\mathcal{E}$ to be transferred to the next chain site. For instance, $\Delta\mathcal{E}=0.57$ if $g=1$ and $\Delta\mathcal{E}=0.04$ for $g=10$. For weak couplings g, the kink (antikink) propagates like the Brownian particle, carrying out thermally activated jumps over the barriers of the PN relief. When the coupling g is sufficiently strong ($g\geqslant 100$), the PN relief is practically absent. In this case, the kink can propagate with permanent velocity and profile.

IV. NONZERO TEMPERATURE KINK DYNAMICS IN THE DISPLACIVE LIMIT

In the *displacive* limit (for the chains with strong interparticle coupling, e.g., $g\geqslant 100$), the kinks (and antikinks) can propagate with permanent velocity and shape. In the unthermalized chain ($D=0$) with $\gamma=0$ and $f=0$, both the directions of soliton motion are completely equivalent. However, due to the asymmetry of the kink (antikink) profile as mentioned in the preceding section, some specific (asymmetric) properties of the interaction between the kink being placed to the left and the antikink being placed to the right compared to the opposite situation might appear. Clearly, there is no difference in this interaction in the case of any symmetric function $V(u)$. Let us find the effective potentials of both these interactions, which we denote by E_{AK} (if the antikink is situated to the left, whereas the kink is found to the right) and E_{KA} in the opposite case. Obviously, $E_{AK}=E_{KA}$ for a symmetric potential $V(u)$.

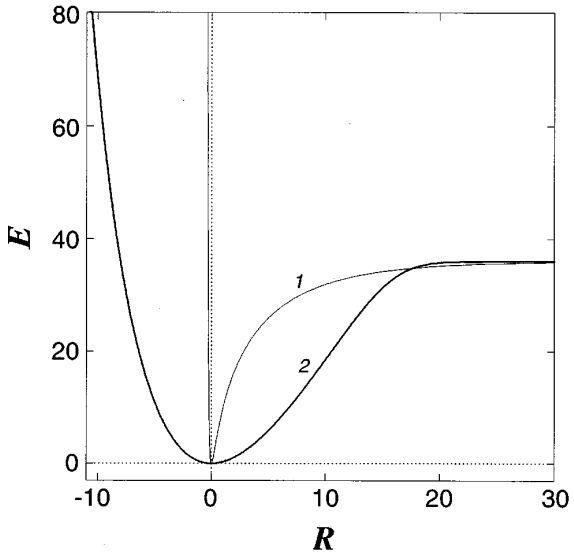

FIG. 4. Effective potential of the interaction of the antikink with the kink [$E_{AK}(R)$, curve 1] and of the kink with the antikink [$E_{KA}(R)$, curve 2] in the chain with $g=256$, $b_1=0.5$, and $b_2=5$.

To find each of these effective potentials, we solve the minimization problem (10) with the conditions that fix the boundary particles either in the left (KA interaction) or in the right (AK interaction) well and additionally the middle particle of the chain [say, the $(N/2)$th particle] is supposed to be fixed. Thus, for the AK interaction we define the boundary conditions as $u_1=u_N=1$ and fix a certain value of the displacement $u_{N/2}$. Let $\{u_n^0\}_{n=1}^N$ be a solution of this minimization problem. Varying then the displacement values $u_{N/2}$ from $-1+0$ to $+\infty$, we can study the dependence of the interaction energy E_{AK} on the distance between the antikink and kink defined by

$$R=R_{AK}=\frac{1}{2}\sum_{n=1}^{N}(1-u_n^0). \tag{13}$$

When $u_n^0=1$, we have $E_{AK}=0$ and the distance $R_{AK}=0$. When $u_{N/2}\to -1+0$, the energy $E_{AK}\to 2E_0$ and the distance $R_{AK}\to+\infty$, where E_0 is the energy of the standing kink (or antikink). Next, $E_{AK}\to+\infty$ and $R_{AK}\to-\infty$ if $u_{N/2}\to+\infty$.

To find the interaction energy E_{KA}, we have to solve the same problem (10), but with the boundary conditions $u_1=u_N=-1$. In this case, we vary the displacement $u_{N/2}$ from $+1-0$ to $-\infty$. Now the distance between the kink and antikink is given by

$$R=R_{KA}=\frac{1}{2}\sum_{n=1}^{N}(1+u_n^0). \tag{14}$$

In this case, $E_{KA}\to 2E_0$ and $R_{KA}\to+\infty$ if $u_{N/2}\to+1-0$. At $u_{N/2}=-1$, we have $E_{KA}=0$ and $R_{KA}=0$. Also, $E_{KA}\to+\infty$ and $R_{KA}\to-\infty$ if $u_{N/2}\to-\infty$.

The minimization problem (10) was solved for both the AK and KA interactions at the following chain parameters: $g=256$, $N=500$, $b_1=0.5$, and $b_2=5$. The effective potentials $E_{AK}(R)$ and $E_{KA}(R)$ are plotted in Fig. 4. As follows

from this figure, the asymmetry of the double-well potential results in an essential difference in the form of these potentials. Such a difference should give rise to a different scenario of the AK and KA collision processes.

To study the kink-antikink interaction dynamics, we need to have appropriate initial conditions for the simulations of the equations of motion (7) for the case when the chain is isolated, i.e., $f=0$, $\gamma=0$, and $\eta_n\equiv 0$. We look for solitary wave solutions of permanent profile that are sufficiently smooth from site to site and propagate with a constant velocity s. In this case, setting $u_n(\tau)=u(n-s\tau)$, we can approximately substitute the time derivative $u_n''(\tau)$ in Eq. (7) by the spatial difference derivative $s^2(u_{n+1}-2u_n+u_{n-1})$. As a result, we obtain the discrete algebraic equation

$$(s_0^2-s^2)(u_{n+1}-2u_n+u_{n-1})-V'(u_n)=0, \qquad (15)$$

where $s_0=\sqrt{g}$ is the velocity of small-amplitude waves. Therefore, soliton solutions to Eq. (15) can be found by minimization of the corresponding $(N-2)$-dimensional Lagrangian function

$$\mathcal{L}=\mathcal{L}\{u_n;s\}=\sum_{n=1}^{N}\left[\frac{1}{2}(s_0^2-s^2)(u_{n+1}-u_n)^2+V(u_n)\right] \qquad (16)$$

over all the variables $u_2,\ldots,u_{N-1}$ and fixing the appropriate boundary conditions $u_1=-1$ and $u_N=1$ for a kink and $u_1=1$ and $u_N=-1$ for an antikink.

Let $\{u_n^0\}$ be a solution obtained under the minimization of the function (16). Then

$$u_n'(\tau)=-s(u_{n+1}^0-u_n^0) \qquad (17)$$

is the velocity of the nth particle and

$$\mathcal{E}=\sum_{n=1}^{N-1}\left[\frac{1}{2}(s_0^2+s^2)(u_{n+1}^0-u_n^0)^2+V(u_n^0)\right] \qquad (18)$$

is the soliton energy. The soliton width $\mathcal{D}$ is defined by the same equations (11) and (12). According to these equations as well as Eqs. (17) and (18), we calculated the dependence of the energy $\mathcal{E}$ and the width $\mathcal{D}$ on the velocity s, $0\leqslant s<s_0$. We have obtained that with the growth of the velocity s, the energy $\mathcal{E}$ increases monotonically and the width $\mathcal{D}$ decreases monotonically. As $s\to s_0=\sqrt{g}$, we have $\mathcal{E}\to\infty$ and $\mathcal{D}\to 1$.

Using the results of the minimization of the Lagrangian (16), we carried out simulations of the AK and KA collisions in the chain with $N=500$ and $g=256$. These simulations have shown that the KA collision results in the kink-antikink recombination for velocities $s\leqslant 0.6s_0$ and their elastic reflection if $s\geqslant 0.7s_0$. On the other hand, the AK collision was shown to result in only antikink-kink recombination processes.

V. STOCHASTIC DYNAMICS OF THE CENTRAL PARTICLE OF A KINK

Let us assume now that an initially prepared standing kink (or antikink) state is subjected to the action of a stochastic bath and damping through the coupled stochastic equations of motion (7). Consider only the *central* particle of the kink (or antikink). On the one hand, this particle moves in the asymmetric potential $V(u)$ and, on the other hand, it is coupled to its adjacent nearest-neighboring particles. Clearly, the central particle at a given instant of time can be considered as moving in some effective double-well potential $U(u)$ as shown in Fig. 5(a), which depends on the bias force f and the interparticle coupling parameter g. This potential can be calculated explicitly and the procedure resembles that of calculating the PN relief. Initially, by solving the minimization problem (10) for a kink or an antikink, we fix the two stable kink (or antikink) configurations of the variables $u_1,\ldots,u_N$, which are simply shifted by one period of the PN relief. Let the first configuration correspond to the case when the $(N/2)$th particle is situated around the left well of the potential $V(u)$ and the second one when this particle is in the vicinity of the right well [the latter case is shown schematically in Fig. 5(b)]. Then we vary continuously the $u_{N/2}$th displacement, keeping the rest of the variables in each of the two kink (or antikink) states. As a result, we get two different effective potentials $U_1(u)$ and $U_2(u)$ for the $(N/2)$th particle being placed in the left and the right well, respectively. Obviously, each of these potentials has a double-well form if the coupling g is not very large (discrete regime), but the depth of the left well of $U_1(u)$ and that of the right well of $U_2(u)$ will be different, in general. Finally, ''sewing'' these wells (the left half of U_1 and the right half of U_2) at their barrier tops, we obtain the effective potential $U(u)$, which appears to be *nondegenerate*, since the depth of the left well of U_1 differs from that of the right well of U_2. As follows from Fig. 5(a), the right (low-frequency)

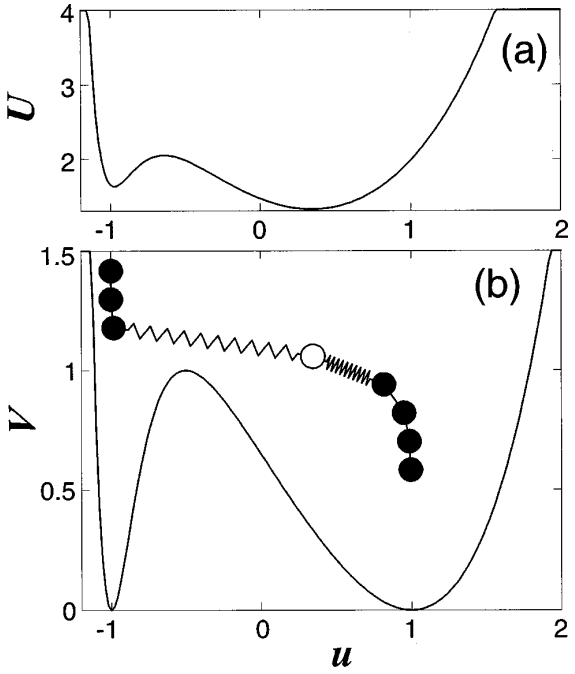

FIG. 5. Results of calculations for the central particle of an antikink at $g=1$: (a) the double-well form of the effective potential $U(u)$ with nondegenerate local minima and (b) the schematic representation of the corresponding antikink solution with the central particle (white ball) located in the right well of the on-site potential $V(u)$.

minimum now becomes a ground state with the lowest energy: $U(l_1)>U(l_2)$. The local minima at $u=l_i$ labeled by the index i, $i=1$ (left) and $i=2$ (right), as well as the barrier top position l_0 of the ''dressed'' potential $U(u)$ are displaced from the corresponding stationary points of the ''bare'' potential $V(u)$, as can be seen by a comparison of Figs. 5(a) and 5(b). Note that the nondegeneracy of the potential $U(u)$ is due to the asymmetry of the potential $V(u)$, while for a symmetric function $V(u)$ the corresponding potential $U(u)$ is always symmetric. The frequencies of small-amplitude oscillations at the local minima given by $\omega_{1,2}=\sqrt{U''(l_{1,2})}$ are also different and their difference vanishes with the growth of the coupling g. On the other hand, the dressed frequencies ω_i tend to the bare frequencies Ω_i defined through the on-site potential $V(u)$ if $g\to 0$. As a result of the linearization around each of these local minima, two parabolic potentials arise with the frequencies ω_i. Due to the frequency disparity and nondegeneracy, the residence probability of the central particle in each local minimum of the effective potential $U(u)$ will be different. We evaluate the relative residence probabilities by using the Kramers theory and use the term ''stochastic ground state'' to refer to the minimum where the particle spends more time or has an averaged residence probability exceeding 1/2.

Let p be the probability of finding the central particle in the left minimum. Besides the ratio ω_1/ω_2, this probability depends on the noise intensity D and correlation time τ_c. In order to investigate the dependence of p on these parameters, we consider the effective single-particle equation for stochastic oscillations of the $(N/2)$th particle in each parabolic potential well. Denote the stochastic field $u_{N/2}-1$ by $\overline{u_1}$ and $u_{N/2}+1$ by $\overline{u_2}$. Then, according to Eq. (7), the linearized stochastic equation for the central particle becomes

$$\overline{u}''_{1,2}+\omega_{1,2}^2\overline{u}_{1,2}+\gamma\overline{u}'_{1,2}=\eta, \tag{19}$$

where the random force $\eta(\tau)$ satisfies the corresponding single-particle covariance given by [see Eq. (8)]

$$\langle \eta(\tau_1)\,\eta(\tau_2)\rangle = 2D\gamma\varphi(\tau_1-\tau_2). \tag{20}$$

Using Eqs. (19) and (20), the total (kinetic and potential) averaged energy of the stochastic oscillations in each well $(i=1,2)$ can be represented as the sum

$$\langle E_i\rangle = K_i+P_i=\lim_{\tau\to\infty}\frac{1}{\tau}\int_0^\tau\left[\frac{1}{2}\,(\overline{u}_i')^2+\frac{1}{2}\,\omega_i^2\overline{u}_i^2\right]d\tau$$

$$=D\gamma\int_{-\infty}^{\infty}(\omega^2+\omega_i^2)|R_i(\omega)|^2F(\omega)\,d\omega,\quad i=1,2, \tag{21}$$

where

$$R_{1,2}(\omega)=\frac{1}{\omega_{1,2}^2-\omega^2-i\gamma\omega} \tag{22}$$

is the response function of the Langevin equation (19) and the Fourier transform is defined by

$$F(\omega)=\frac{1}{2\pi}\int_{-\infty}^{\infty}\varphi(\tau)e^{-i\omega\tau}d\tau. \tag{23}$$

For the exponentially correlated noise defined by Eq. (9), the Fourier transform is simply the Lorentzian

$$F(\omega)=\frac{\lambda^2}{2\pi(\lambda^2+\omega^2)}. \tag{24}$$

Using the explicit expressions (22) and (24), by straightforward contour integration we find the averaged values of the kinetic energy

$$K_i=\frac{1}{2}\,D\,\frac{\lambda^2}{\lambda^2+\lambda\gamma+\omega_i^2} \tag{25}$$

and of the potential energy

$$P_i=\frac{1}{2}\,D\,\frac{\lambda^2(\lambda^2-\gamma^2+\omega_i^2)+\lambda\gamma\omega_i^2}{(\lambda^2+\omega_i^2)^2-\gamma^2\lambda^2}. \tag{26}$$

In the limiting case of infinitely small frictions ($\gamma\simeq 0$), the expressions (25) and (26) are essentially simplified, so that the total averaged energy becomes

$$\langle E_{1,2}\rangle = D\lambda^2/(\lambda^2+\omega_{1,2}^2). \tag{27}$$

The expression (27) together with the depths $\Delta U_i=U(l_0)-U(l_i)$, $i=1$ (left) and $i=2$ (right), allows one to determine which well of the on-site potential $V(u)$ is visited more often by the particle, being the stochastic ground state at given values of D and λ. As a result, we obtain the dependence of the left (right) well residence probability on the correlation time τ_c. Indeed, the rate of the particle transfer from the left ($i=1$) or right ($i=2$) minimum to the other one is

$$p_i=\frac{\omega_i}{2\pi}\,\exp\left[-\frac{\Delta U_i}{\langle E_i\rangle}\right]. \tag{28}$$

Therefore, the probability of finding the particle in the left well is

$$p=\frac{1}{1+A},$$

$$A=\frac{p_2}{p_1}$$

$$=\frac{\omega_1}{\omega_2}\,\exp\left[-\frac{\Delta U_1-\Delta U_2+(\omega_1^2\Delta U_1-\omega_2^2\Delta U_2)\,\tau_c^2}{D}\right]. \tag{29}$$

We note that when $A=1$ both the minima are probable equally ($p=1/2$); using this property, we can find analytically the critical noise correlation time τ_0 that signals the *reversal* of the stochastic ground states:

$$\tau_0=\sqrt{\frac{D\ln(\omega_1/\omega_2)-(\Delta U_1-\Delta U_2)}{\omega_1^2\Delta U_1-\omega_2^2\Delta U_2}}. \tag{30}$$

The value τ_0 determines the correlation time, for values larger (smaller) of which the left (right) potential minimum becomes more probable. As a result, the left (right) minimum is a stochastic ground state for $\tau_c > \tau_0$ ($\tau_c < \tau_0$). At zero noise strength ($D=0$) and without a bias field ($f=0$), the right (low-frequency) well is always a stochastic ground state ($\tau_0 = 0$). At nonzero noise strengths, a ''freezing'' of high-frequency oscillations occurs when $\tau_c > 0$ and this effect is stronger for the left (high-frequency) well. As a result, the probability p of finding the particle in the left minimum increases with the growth of the noise correlation time τ_c, reaching the value 1/2 at $\tau_c = \tau_0$ and exceeding it for all $\tau_c > \tau_0$.

Thus, having calculated the effective potential $U(u)$ (in fact, we need to know only the effective frequencies $\omega_{1,2}$ and depths $\Delta U_{1,2}$), we can conclude which (left or right) well is a stochastic ground state. In other words, one can determine the direction of preferential particle transfers over the barrier separated by the minima of the on-site potential $V(u)$. This knowledge (about the residence probability of the central particle) immediately allows one to determine the direction of the drift of the kink as a whole object. Indeed, when a kink propagates to the right (left) end of the chain, its central particle is transferred from the right (left) well to the left (right) one. The opposite situation with the directions holds for an antikink. Summarizing, one can conclude that the direction of motion of the central particle is opposite (along) the direction of the kink (antikink). Therefore, if the reversal of the stochastic ground state for the central particle occurs, then the corresponding reversal effect takes place for the kink and antikink motion. For a given τ_c, only one of the minima is more probable and therefore it becomes the corresponding stochastic ground state; this leads to the *directed* kink motion, i.e., to symmetry breaking the Brownian motion of kinks and antikinks. Furthermore, this analysis shows that kinks and antikinks propagate in *opposite* directions, respectively. Thus, varying the noise properties such as the correlation time τ_c or the strength D, the reversal of the stochastic ground state occurs, leading to the reversal of the direction of kink (antikink) propagation. Note that, according to Eq. (30), the reversal time τ_0 depends on the noise strength D. This dependence can be calculated explicitly and some results are given in Table I.

The reversal effect occurs for sufficiently small values of the coupling g since with increasing g, the disparity of the effective frequencies ω_i and the depths ΔU_i decreases and, as a result, the switching (reversal) time τ_0 monotonically tends to infinity [see Eq. (30)]. Hence the cooperativity of the chain *opposes* the reversal effect and for sufficiently large g it disappears, though the double-well form of the effective potential $U(u)$ still exists. More precisely, for $\tau_c < \tau_0$, we have $p(\tau_c) < 1/2$ and, as a result, the kink (antikink) should propagate to the left (right), while for $\tau_c > \tau_0$ we obtain $p(\tau_c) > 1/2$ and now the kink (antikink) should move to the right (left). Indeed, at the values $b_1 = 0.5$ and $b_2 = 5$ we obtained $p(\tau_c) < 1/2$ for all reasonable values of the correlation time τ_c if $g \geqslant 1.5$. Note that for a symmetric double-well potential ($b_1 = b_2$), the probability p is always 1/2 and therefore the stochastic vibrations cannot give rise to a directed kink (antikink) motion.

Thus, in the chain with an on-site AB potential, we have two counterbalancing factors. On the one hand, the interparticle coupling g results in effective increasing the high-frequency minimum of the potential $U(u)$ and this circumstance, in turn gives rise to the decreasing the probability of particle transfers from the low-frequency well to the high-frequency one. Note that in the potential $V(u)$ this probability is always less than 1/2. On the other hand, the presence of a nonzero corellation time τ_c results in effective freezing out high-frequency oscillations and this is exhibited in decreasing the probability of particle transfers from the high-frequency (left) well to the low-frequency (right) one. Therefore, the direction of the noise-induced motion of the kink is determined by these factors. When the coupling g is sufficiently weak, the growth of the correlation time τ_c results in switching the direction of kink motion, but for strong couplings g the kink motion direction does not depend on the correlation time τ_c.

TABLE I. Dependence of the reversal time for the stochastic ground states τ_0 on the noise strength D.

D	τ_0
0.1	0.047
0.2	0.067
0.3	0.082
0.4	0.094
0.5	0.105

VI. NUMERICAL RESULTS

Consider a finite AB chain with fixed ends and consisting of N particles. The chain is assumed to be driven by exponentially correlated noise, including white noise as a particular case, so that its dynamics is described by the set of equations (7)–(9) where $n = 1,2,\ldots,N$. However, for numerical studies of the dynamics of the chain particles driven by colored noise, it is convenient to substitute Eqs. (8) and (9) by the first-order stochastic equations

$$\frac{d\eta_n}{d\tau} = \lambda(\xi_n - \eta_n), \quad n = 0, \pm 1, \pm 2, \ldots, \tag{31}$$

where the $\xi_n(\tau)$'s are normally distributed δ-correlated random forces [21], i.e.,

$$\langle \xi_{n_1}(\tau_1)\xi_{n_2}(\tau_2)\rangle = 2D\gamma\delta_{n_1 n_2}\delta(\tau_1 - \tau_2). \tag{32}$$

First, we consider the stochastic vibrations of the chain in one of the ground states, when $u_n = -1$ or $u_n = 1$ for all $n = 1,\ldots,N$. The asymmetry of the potential $V(u)$ should result in the difference of the dynamics of the chain particles in these ground states. Indeed, the asymmetric ground states have different spectra of small-amplitude oscillations, viz., $[\Omega_i, \sqrt{\Omega_i^2 + 4g}]$, $i = 1,2$. Let us define the dimensionless thermal capacity by $c_i = \langle E_i \rangle / D(N-2)$ for each of the ground states. Note that for the system with harmonic forces and white noise the dimensionless thermal capacity is always 1. The presence of an anharmonicity leads to some depen-

TABLE II. Dependence of the dimensionless thermal capacities $c_{1,2}$ of the ground states $u_n \equiv \mp 1$ on the correlation time τ_c at $g=1$ and $D=0.1$, $g=10$ and $D=0.2$, and $g=100$ and $D=0.2$.

	$g=1,\ D=0.1$		$g=10,\ D=0.2$		$g=100,\ D=0.2$	
τ_c	c_1	c_2	c_1	c_2	c_1	c_2
0.01	1.027	0.975	1.032	0.992	1.002	0.980
0.1	0.550	0.930	0.511	0.815	0.305	0.433
0.2	0.228	0.825	0.200	0.568	0.104	0.219
0.3	0.114	0.731	0.100	0.410	0.050	0.142
0.4	0.069	0.617	0.057	0.309	0.030	0.099
0.5	0.045	0.501	0.038	0.233	0.019	0.076
0.6	0.032	0.415	0.027	0.187	0.013	0.058

dence of $c_{1,2}$ on the noise strength D and the presence of a nonzero correlation time τ_c also implies a dependence on this parameter.

Besides the values $b_1=0.5$ and $b_2=5$, we take throughout the present paper $\gamma=0.1$. We look for the dependence of $c_{1,2}$ on the correlation time τ_c at different values of the coupling g. To this end, we integrate numerically the system of equations (7) and (31) with the correlation equations (32) at the initial conditions $u_n(0)\equiv -1$, $u_n'(0)\equiv 0$ and $u_n(0)\equiv 1$, $u_n'(0)\equiv 0$ with $N=100$ and $f=0$. The results of these simulations are presented in Table II. As follows from these results, at $\tau_c>0$ the right ground state has higher capacity than the left one. The ratio c_2/c_1 increases monotonically with the growth of τ_c. The reason for this behavior is that the spectrum of small-amplitude oscillations at $u_n\equiv 1$ is below the spectrum of oscillations at $u_n\equiv -1$ (see Table III). Therefore, the increase of the correlation time τ_c leads essentially to freezing high-frequency vibrations at the state $u_n\equiv -1$. With increasing the coupling g, the relative shift of the spectra of small-amplitude oscillations is reduced and, as a result, the ratio c_2/c_1 is also decreased. The growth of the coupling g leads to a gradual equalization of the capacities of the ground states ($c_2/c_1 \to 1+0$ when $g\to\infty$).

Consider now the kink dynamics. We choose the initial conditions for the system of equations (7) and (31), which correspond to the stable standing kink (antikink) state, i.e., $u_n(0)=u_n^0$ and $u_n'(0)=0$, where $n=1,2,\ldots,N$ and $\{u_n^0\}_{n=1}^N$ is a solution of the minimization problem (10). First, we fix the central particle of the kink, which is the closest to the top of the barrier l_0, and then simulate Eqs. (7) and (31) during the time interval $\tau=500$. This time is sufficient for the chain to come to thermal equilibrium with the bath, but the kink itself is not yet allowed to move. After this time period, we allow the fixed particle to move and observe the kink motion in the thermalized chain. To this end, we define the kink center n_c as an intersection point on the (n,u) plane of the line connected the points $\{(n,u_n)\}_{n=1}^N$ with the line $u=u_0$.

TABLE III. Dependence of the spectra of small-amplitude oscillations $[\Omega_i, \sqrt{\Omega_i^2+4g}]$, $i=1,2$, on the interparticle coupling g.

g	Ω_1	$\sqrt{\Omega_1^2+4g}$	Ω_2	$\sqrt{\Omega_2^2+4g}$
0	9.23	9.23	1.46	1.46
1	9.23	9.44	1.46	2.48
10	9.23	11.19	1.46	6.49
100	9.23	22.03	1.46	20.05

The existence of the reversal of soliton motion predicted through the analytical arguments of Sec. V was confirmed by the numerical simulations for the parameter values $N=100$, $g=1$, $D=0.2$, and $f=0$. Their results are illustrated in Fig. 6. In the simulations we observed that at small g, the kink and antikink are mainly standing and only very rarely do they jump randomly to the nearby lattice sites. At small correlation times τ_c, including also white noise ($\tau_c=0$), the contact with the thermal bath moves the kink (antikink) to the left (right) as shown by path 1 (2) in Fig. 6. An increase in the noise correlation time τ_c results in a change in the direction of their motion as demonstrated by paths 3 and 4 in Fig. 6. This behavior of kinks and antikinks is in agreement with the results of Sec. V, where we have predicted the reversal of the stochastic ground state of the chain with sufficiently weak interparticle coupling g at a certain value of the correlation time τ_c. This behavior is explained by the stronger freezing (with the increase of τ_c) of the high-frequency state $u_n\equiv -1$ compared to that of the low-frequency state $u_n\equiv 1$ (see Table II).

However, in the case of stronger cooperativity ($g=10$), the numerical simulations of Eqs. (7) and (31) with $f=0$ have demonstrated the absence of the reversal effect. Thus the kink (antikink) propagation is directed only to the left (right), independently on the correlation time τ_c. In this case, the growth of τ_c results only in the gradual reduction of the averaged kink velocity, not reaching the reversal effect. The antikink motion for this case is shown in Fig. 7. Again, these results are in agreement with the theory given in Sec.

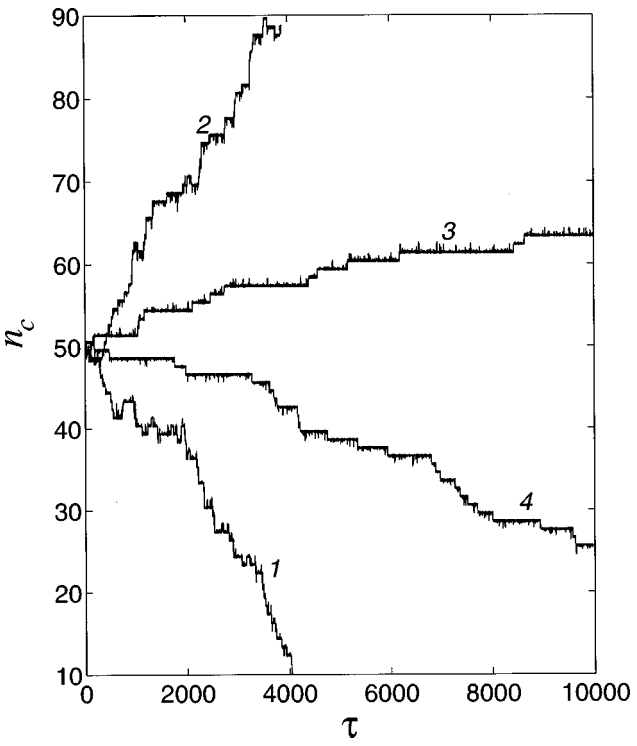

FIG. 6. Noise-induced motion of a kink (curves 1 and 3) and an antikink (curves 2 and 4) in the chain with $N=100$, $g=1$, $b_1=0.5$, $b_2=5$, $\tau_r=10$, $\beta=0.2$, and $f=0$ at $\tau_c=0$ (curves 1 and 2) and $\tau_c=0.3$ (curves 3 and 4).

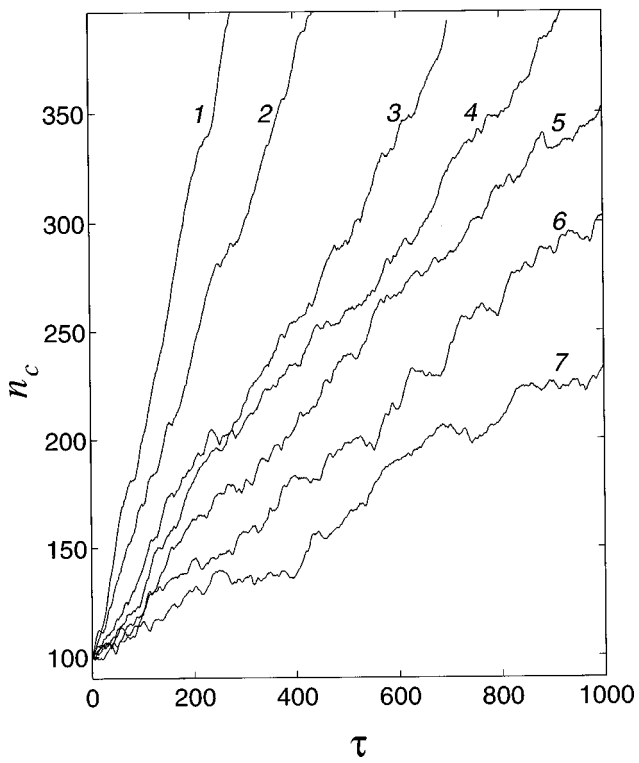

FIG. 7. Noise-induced motion of an antikink ($N=400$, $g=10$, $b_1=0.5$, $b_2=5$, $\tau_r=10$, $\beta=0.2$, and $f=0$) at $\tau_c=0$, 0.1, 0.2, 0.3, 0.4, 0.5, and 0.6 (curves 1, 2, 3, 4, 5, 6, and 7, respectively).

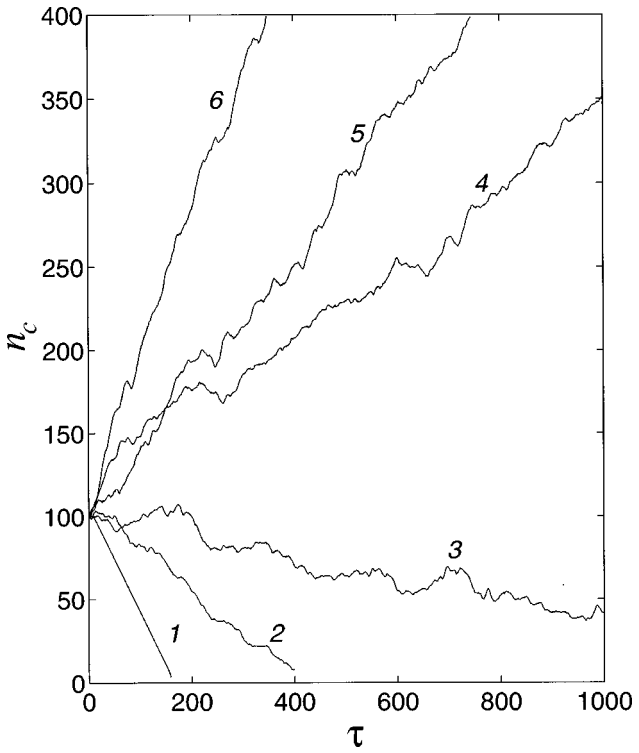

FIG. 8. Thermally activated motion of an antikink at the presence of an external force $f=-0.05$ in the chain with $N=400$, $g=10$, $b_1=0.5$, $b_2=5$, $\tau_r=10$, and $\tau_c=0$ (white noise) at temperatures $D=0$, 0.05, 0.1, 0.15, 0.2, and 0.3 (curves 1, 2, 3, 4, 5, and 6, respectively).

V. Note that with an increase of the coupling g, the effect of the stronger freezing of the high-frequency ground state than of the low-frequency one, which provides at $g=1$ the change of the direction of motion, is reduced (see Table II). The velocity of noise-induced kink motion is increased with a decrease of the correlation time τ_c.

When a constant driving force f is present, the minima of the total on-site potential $V(u)-fu$ become nondegenerate. We consider the case of sufficiently strong cooperativity (e.g., $g=10$) when the reversal associated with varying g is absent. White noise is considered as a particular case. Then, if $f>0$, a kink (antikink) moves along the field, i.e., the kink (antikink) propagates to the left (right) at any noise strength D. Similarly, in the case $f<0$, but for sufficiently small noise strengths D, the soliton motion occurs along the field f. However, with increasing D, this motion becomes slower and slower and at a certain critical temperature $D_0(f)$ the soliton comes to a stop. A further increase of the noise strength gives rise to the kink motion in the opposite direction, i.e., *against* the applied dc force f. As follows from Eqs. (29), even in the limiting case of white noise ($\tau_c=0$), the soliton motion can occur against the field f. The presence of the asymmetry $\omega_1\neq\omega_2$ appears to be a sufficient condition for soliton propagation against an external dc field. In the case of the antikink dynamics, this reversal effect is illustrated in Fig. 8. Here, at $f=-0.05$, $\tau_c=0$, and the noise strengths $D=0,0.05,0.1$, the antikink propagates to the left, while for the values $D=0.15,0.2,0.3$, it moves to the right. We note that kinks or antikinks can propagate against the driving dc force f only if the external force does not exceed a certain threshold value $f_0(D)$. Thus we have observed (see Fig. 9) that at $D=0.2$ and $\tau_c=0$, the antikink propagates to

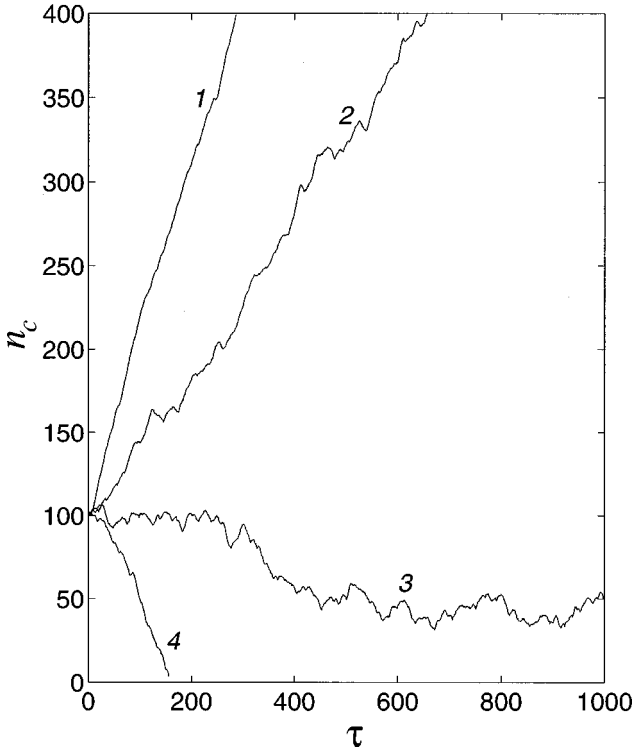

FIG. 9. Same motion [$N=400$, $g=10$, $b_1=0.5$, $b_2=5$, $\tau_r=10$, $\tau_c=0$ (white noise), and $D=0.2$] under the external force $f=0$, -0.05, -0.1, and -0.15 (curves 1, 2, 3, and 4, respectively).

the right (against the driving force f) if $f=0,-0.05$ and to the left (along the field f) if $f=-0.1,-0.15$.

VII. SUMMARY AND OUTLOOK

The reversal of the directed diffusive soliton motion in the kink-bearing model with the on-site potential of an asymmetic double-well form was shown to appear due to two counterbalancing factors. On the one hand, the interparticle coupling results in an effective lifting of the high-frequency minimum of the on-site potential and this in turn gives rise to a decrease of the probability for the particle transfers from the low-frequency well to the high-frequency one. Note that this probability is always less than 1/2 if the chain particles are driven by white noise. On the other hand, the nonzero correlation noise results in effective freezing out high-frequency oscillations and this is exhibited in the decreasing probability of the particle transfers from the left well to the right one. Therefore, the direction of the noise-activated soliton motion is determined by these factors. It is worth mentioning that the reversal of the directed soliton motion can also be induced by other counterbalance factors. Thus, for particular shapes of the asymmetric periodic potential the reversal effect has been observed recently for the single-particle motion [17]. In this case, the change of the current is caused by specific shapes of the ratchet periodic potential or, more precisely, by the proper interplay of its higher derivatives.

The collective effect of rectifying the soliton motion that was shown to be induced by a noise correlation and the strength on topological solitons is generic and not particularly sensitive to the on-site potential details. It is necessary for the effect to take place to have an on-site potential degeneracy accompanied by some potential asymmetry. We found that in the case of asymmetric double wells, kinks and antikinks move in opposite directions even in the presence of white noise, while colored noise of sufficient correlation results in direction reversal. Therefore, the asymmetry of the double-well potential is a sufficient ingredient for directed soliton transport. The kink motion in the presence of white noise does not contradict the second law of thermodynamics since the initial states are not in equilibrium and the kinks can travel only once through the system. In a finite periodic lattice an initially created kink-antikink pair would travel in opposite directions and self-annihilate after reencountering each other, bringing thus the lattice into thermal equilibrium. The effects presented are relevant when ambient temperature is much smaller than the soliton bindiny energy; a number of interesting questions arise if we consider higher temperatures where kink-antikink annihilation and nucleation take place [22,23].

The soliton reversal effect can have a variety of applications in kink-bearing systems with some on-site asymmetry. Thus the contact with a thermal bath can either speed up or slow down transport processes or even reverse them at certain critical values of temperature. Such a high sensitivity of transport mechanisms to temperature can be used by a biosystem for its thermal control. For instance, lowering temperature can result in a charge current for the transformation of chemical into thermal energy. Thus one can conclude that taking into account the realistic asymmetry of biomolecular systems might help in understanding the primary mechanisms of their functioning.

ACKNOWLEDGMENTS

The work was carried out with the financial support from the European Economic Community under the INTAS Grant No. 94-3754. A.V.S. and A.V.Z. are indebted to the hospitality of the Physics Department of the Crete University and the Research Center of Crete where the main part of this work was carried out.

[1] J. A. Krumhansl and J. R. Schrieffer, Phys. Rev. B **11**, 3535 (1975).
[2] S. Aubry, J. Chem. Phys. **62**, 3217 (1975); **64**, 3392 (1976).
[3] For a review see, e.g., A. R. Bishop, J. A. Krumhansl, and S. E. Trullinger, Physica D **1**, 1 (1980).
[4] J. F. Nagle, M. Mille, and H. J. Morowitz, J. Chem. Phys. **72**, 3959 (1980).
[5] M. V. Satarić, J. A. Tuszyński, and R. B. Žakula, Phys. Rev. E **48**, 589 (1993).
[6] A. Ajdari and J. Prost, C. R. Acad. Sci. Ser. 2, **315**, 1635 (1992).
[7] M. O. Magnasco, Phys. Rev. Lett. **71**, 1477 (1993); **72**, 2656 (1994).
[8] C. R. Doering, W. Horsthemke, and J. Riordan, Phys. Rev. Lett. **72**, 2984 (1994).
[9] J. Prost, J.-F. Chauwin, L. Peliti, and A. Ajdari, Phys. Rev. Lett. **72**, 2652 (1994); J.-F. Chauwin, A. Ajdari, and J. Prost, Europhys. Lett. **27**, 421 (1994).
[10] R. D. Astumian and M. Bier, Phys. Rev. Lett. **72**, 1766 (1994).
[11] M. Millonas and M. I. Dykman, Phys. Lett. A **185**, 65 (1994).
[12] F. Julicher and J. Prost, Phys. Rev. Lett. **75**, 2618 (1995).
[13] T. Dialynas and G. P. Tsironis, Phys. Lett. A **218**, 292 (1996).
[14] D. W. McLaughlin and A. C. Scott, Phys. Rev. A **18**, 1652 (1978).
[15] F. Marchesoni, Phys. Rev. Lett. **77**, 2364 (1996).
[16] A. V. Savin, G. P. Tsironis and A. V. Zolotaryuk, Phys. Lett. A (to be published).
[17] R. Bartussek, P. Reimann, and P. Hänggi, Phys. Rev. Lett. **76**, 1166 (1996).
[18] A. V. Zolotaryuk, St. Pnevmatikos, and A. V. Savin, Physica D **51**, 407 (1991).
[19] X. Duan and S. Scheiner, J. Mol. Struct. **270**, 173 (1992).
[20] See, e.g., M. Peyrard and M. Remoissenet, Phys. Rev. B **26**, 2886 (1982).
[21] K. Lindenberg, B. J. West, and G. P. Tsironis, Rev. Solid State Sci. **3**, 143 (1989).
[22] M. Büttiker, Z. Phys. B **68,** 161 (1987).
[23] M. Büttiker and T. Christen, Phys. Rev. Lett. **75,** 1895 (1995).